Drift probabilities for Icelandic cod larvae

David Brickman, Gudrun Marteinsdottir, Kai Logemann, and Ingo H. Harms

Brickman, D., Marteinsdottir, G., Logemann, K., and Harms, I. H. 2007. Drift probabilities for Icelandic cod larvae – ICES Journal of Marine Science, 64, 49–59.

The climatological distribution of juvenile Icelandic cod is characterized by a negative spatial age gradient, with a fairly abrupt decrease in age near the northwest corner of Iceland, and a spatial abundance gradient with higher concentrations of 0-group fish inshore. Flowfields from a high-resolution circulation model developed for Icelandic waters were used to investigate larval drift from the various spawning grounds in Icelandic coastal waters to understand the distribution of 0-group fish. To present the results clearly, drift probability density functions (pdfs) are derived describing the probability of drifting from a given spawning ground to a given spatial region over a specified time interval. These pdfs are used to determine the spawning grounds most probably contributing to the observed age distribution. The observed spatial gradient in age is likely due to differences in the spawning location of larvae, with older larvae originating in spawning grounds in the southwest and younger larvae from farther north. In general, the contribution from the main spawning grounds in the southwest is predicted to decrease with clockwise distance from the source region. The pdf technique was also used to investigate drift from regions on the south coast of Iceland corresponding to known or possible subpopulation spawning grounds, to see whether these spawning areas are associated with distinct drift patterns. This technique is a useful way to present larval drift results and to facilitate comparison with real data.

Keywords: Iceland circulation, larval drift, probability density function, subpopulations.

Received 16 December 2005; accepted 11 September 2006; advance access publication 10 November 2006.

D. Brickman: Department of Fisheries and Oceans, PO Box 1006, Dartmouth, Nova Scotia, B2Y 4A2, Canada. D. Brickman: Marine Research Institute, Skulagata 4, 121 Reykjavik, Iceland. G. Marteinsdottir: Institute of Biology, University of Iceland, Sturlugata 7, 101 Reykjavik, Iceland. K. Logemann and I. H. Harms: University of Hamburg, Institute of Oceanography, Troplowitzstrasse 7, D22529, Hamburg, Germany. Correspondence to D. Brickman: tel: +1 902 4265722; fax +1 902 4266927; e-mail: brickmand@dfo-mpo.gc.ca.

Introduction

The Icelandic cod stock has suffered from heavy exploitation pressure, leading to a gradual decline in biomass, since the middle of the last century (Marteinsdottir *et al.*, 2005). Today its biomass is ~35% of what it was in 1950. Recruitment was generally high though variable in the 1970s and 1980s, but now it is low, with little variability. Because of the importance of the cod stock to Iceland's economy, extensive studies have been carried out to understand its fluctuations and to aid in its management. Data collected include more than 20 years of adult spawning and feeding ground surveys, plus 35 years of pelagic 0-group sampling. As a result, a general picture of the distribution of adult and young cod has been developed (Begg and Marteinsdottir, 2000, 2003; Saemundsson, 2005).

Biophysical models use information on spawning-stock distribution and flowfields to simulate the drift, growth, and mortality of eggs and larvae (Heath and Gallego, 1998; Brickman and Frank, 2000; Hinrichsen *et al.*, 2002). A key component of this modelling concerns the drift of the eggs and larvae, based on circulation-model flowfields. Until recently, no high-resolution physical modelling had been done specific to drift around Iceland, so knowledge of characteristic larval drift pattern (Begg and Marteinsdottir, 2000) was speculative. As part of the METACOD project (an EC fifth framework research project), a circulation model was developed for Icelandic (and Scottish) waters. The present study uses flowfields from that model to investigate larval drift from the various spawning grounds around Iceland's coasts.

Begg and Marteinsdottir (2000) presented 29 years (1970–1998) of larval 0-group data in terms of the spatial distribution of age and abundance. Their analysis included a climatological (i.e. averaged) picture based on dividing the area around Iceland into eight regions. A key finding of Marteinsdottir *et al.* (2000a), confirmed by Begg and Marteinsdottir (2000), was a clockwise (negative) spatial age gradient starting from the main spawning grounds in the southwest (region 1; Figure 1), and a fairly abrupt decrease in age at the boundary of regions 2 and 3 along Iceland's northwest coast (Figures 1 and 2). Also notable (Figure 1) were a general decrease in abundance on the shelf moving from shallow to deep waters, a pattern of older larvae in low abundance between Iceland and Greenland (region 8, or R8), and a bimodal distribution of age along the south coast (Figure 2; R7). Begg and Marteinsdottir (2000) analysed these results from the perspective of the likelihood that the age distribution in a given region originated in larvae spawned in region R1. One of the main objectives of this paper is to revisit these results using particle tracking to help understand the observed distributions. Specifically, we use particle tracking starting from the various spawning grounds to determine the most likely contributors to the observed age distribution in a given region.

Recent genetic and tagging studies revealed interesting features of the spawning populations on the south coast. Jonsdottir *et al.* (2002) found a genetic difference at the Syp-I locus (=Pan-I) between spawning cod collected at two locations separated by a

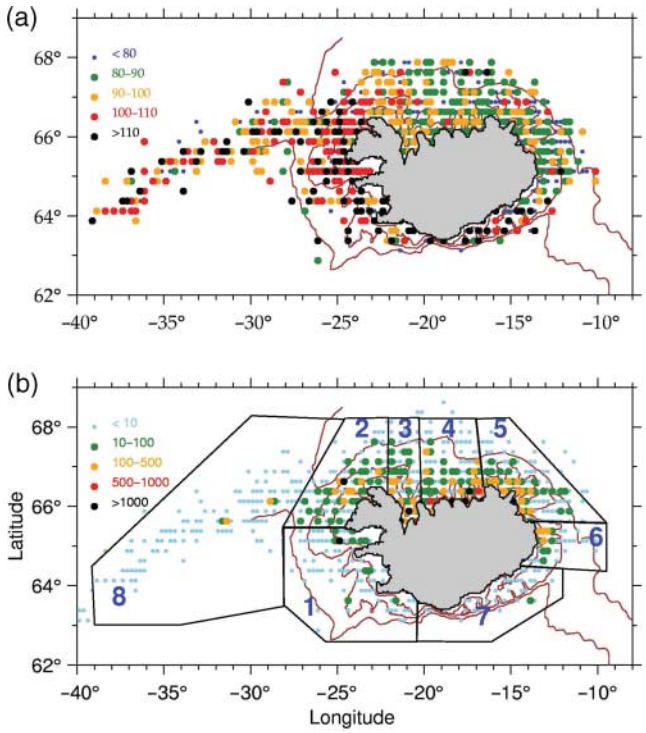

Figure 1. Climatological survey data for 0-group cod around Iceland averaged over the years 1970–1998, on a 0.25 × 0.25° grid. (a) Age (d). (b) Abundance (number per kilometre towed). The eight regions used by Begg and Marteinsdottir (2000) are indicated on (b), and the 100, 200, and 600 m isobaths are shown on this and subsequent figures.

distance of 50 nautical miles. However, Pan-I suffers from directional selection in gadoids (Pogson, 2001; Canino and Bentzen, 2004), so the genetic differences may indicate the presence of aggregations of distinct life histories rather than genetically isolated groups. Palsson and Thorsteinsson (2003), using data storage tags, inferred a distinct difference in the migration patterns of fish tagged on the main spawning ground, one group remaining in warm shallow whereas while another followed a deeper, colder migration route. Marteinsdottir *et al.* (2000b) and Petursdottir *et al.* (in press) found a correlation between size, growth, and depth of spawners on the main spawning grounds, with larger, faster-growing fish occupying shallower water. Jónsdóttir *et al.* (2006) identified three groups of spawners (north, south–shallow, and south–deep) based on otolith morphology. A basic life history question is how juveniles from distinct populations recruit to their respective adult spawning groups. Heeding this question, we investigate whether larvae released from the various possible (subpopulation) spawning grounds on the south coast have distinct drift histories. In other words, are the genetic/behavioural/phenotypic differences found in adult populations related to different drift histories of larvae spawned by these populations?

Data

The data, the same used by Begg and Marteinsdottir (2000), consist of 29 years (1970–1998) of pelagic 0-group surveys, trawled 20–50 m deep, and containing more than 150 stations per year. Since 1980, a fixed survey route has been used. Abundance (number per nautical mile) and total body length are recorded at each station. The latter are adjusted to the mean survey date [yearday (yd) 232] using a growth rate of 0.65 mm d^{-1} (Marteinsdottir *et al.*, 2000a). Abundance is adjusted to the mean survey date using a mortality rate of 0.03 d^{-1}, consistent with late larval mortality (Houde, 1997). Length data (L, mm) are converted to a total drift age (A, days) using the relationship (Begg and Marteinsdottir, 2000)

$$A = \frac{(L - 15.8723 + 2.5401T)}{(0.4526 + 0.0307T)} + 16, \quad (1)$$

where T is the temperature (°C), and the offset (16) is the average hatching time in Icelandic waters (Begg and Marteinsdottir, 2000). Although the annual temperature relationship given by Begg and Marteinsdottir (2000) could have been used, it was found that for the range of lengths encountered (85% between 30 and 60 mm), and the typical temperature range (6–10°C), use of a constant temperature of 8°C gave a maximum error of <4 days (~8%), so the simpler formula was considered adequate. Climatological mean abundance and age distributions were created by averaging the data across years on a 0.25 × 0.25° grid (Figure 1). The choice of grid size was based on preserving the inherently fine-scale structure of the data while avoiding graininess attributable to spatial oversampling.

Age histograms (Figure 2) were created for each of the eight regions identified by Begg and Marteinsdottir (2000). Definition of the regions was based on a spatial division used in the BORMICON model used to evaluate multispecies interactions in Icelandic waters (Stefánsson and Palsson, 1997). Although not based on an objective analysis, the regional decomposition is useful in that it helps describe the general distributions found in Icelandic waters.

Spawning grounds

Some spawning is thought to take place in most of Iceland's bays and fjords, with the main spawning grounds being in the southwest (region 1; Figure 1) (Marteinsdottir *et al.*, 2000b). The actual selection of locations to release particles was mainly based on fishing logbooks and spawning survey data (Marteinsdottir and Bjornsson, 1999; Marteinsdottir *et al.*, 2000a, b), but had to be somewhat subjective in that precise spawning grounds are not known in all cases nor are they necessarily static entities. In all, 13 spawning grounds were chosen, numbered in a clockwise fashion starting from the main spawning area (Figure 3). Some of these contain, or potentially contain, more than one possible subspawning ground. Because released particles are numbered, it is possible, *a posteriori*, to analyse the drift results from subregions of a given spawning ground.

Circulation model

The origin of the METACOD circulation model is the Hamburg Shelf Ocean Model (HAMSOM) (Backhaus, 1985), previously applied to the region by Harms *et al.* (1999, 2000) and Logemann *et al.* (2004), and recently updated by Harms *et al.* (2003). The current version was modified by KL, and includes horizontally and vertically adaptive grids (Khokhlov, 1998).

The modelling system consists of a North Atlantic/Arctic Ocean model domain with a hierarchy of nested, highly resolved subdomains. The model's vertically adaptive grid allows it to

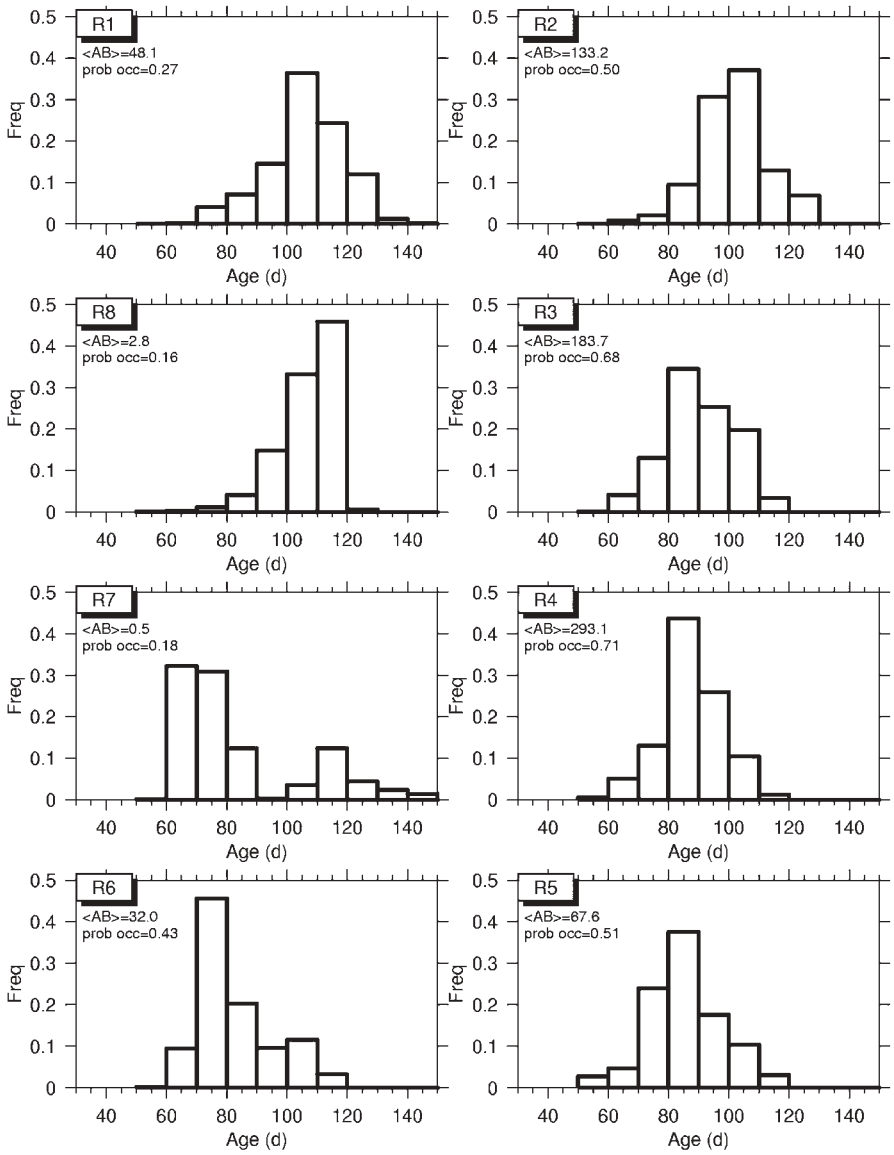

Figure 2. Age histograms for 0-group cod for the eight regions around Iceland. The mean abundance (<AB>, number per kilometre towed) and the probability of occurrence (prob occ, non-zero tows divided by the total number of tows) are indicated. A back-calculated spawning duration curve can be derived by converting age to yd using the formulation yd = 230 − age.

handle complex bathymetries and provides high vertical resolution near or at topographic discontinuities. The coarse base matrix has a resolution of ∼150 km in the subtropical Atlantic and 75 km in the Arctic. The highest resolution is 1.2 km in Icelandic waters (Figure 4). The model is eddy-resolving over much of Iceland's shelf waters.

For spin-up, the model was integrated for 10 years on the coarse base grid. It is initialized with climatological temperature and salinity data from the Polar Science Center Hydrographic Climatology (PHC) world ocean data set (Steele *et al.*, 2001) and forced with the wind stress from the Ocean Model Intercomparison Project data set (Röske, 2001). This data set, based on re-analysis of 15 years of atmospheric data held by the European Centre for Medium Range Weather Forecasting, describes a 360 days cyclic, stationary, climatological year, that includes the passage of storms (i.e. it is a "storm climatology"). During the simulation, the computed ocean temperature and salinity fields were restored with a time constant of 30 days, to the PHC's monthly fields.

Using the cyclic stationary spin-up run as the basic state, the model is run to equilibrium with the high-resolution embedded grids. Seasonal values of run-off were prescribed at the Icelandic coast, based on all accessible geological records. The result is a time-dependent climatological year of flowfields. For more details on the model, and the model performance, see Logemann and Harms (2006).

Model flowfield variables are saved to disk daily, for use by the particle-tracking routine. This routine takes the variable resolution data and interpolates it onto a uniform 1 × 1 km grid, on a subdomain chosen by the user. Because the grid resolution is not user-adjustable, computer memory limits the possible size of the subdomain.

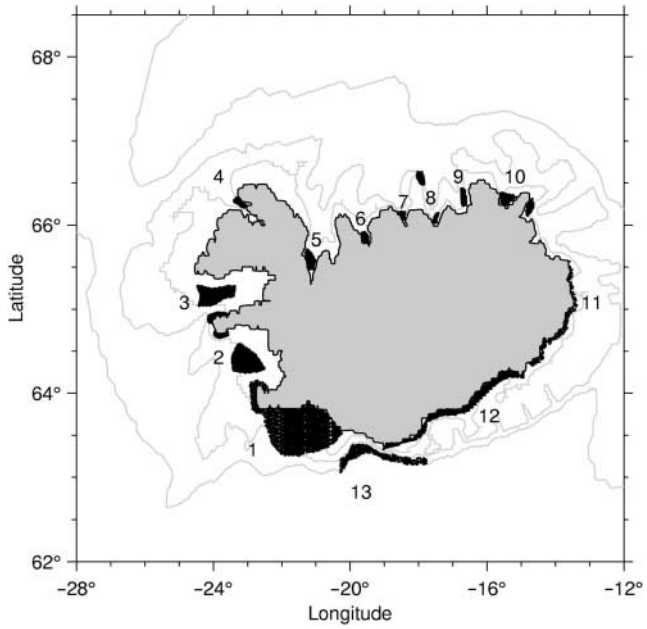

Figure 3. The 13 cod spawning grounds used in this study.

Drift algorithm

In all, 10 000 particles were released from the 13 spawning grounds, distributed roughly in proportion to the surface areas of individual spawning grounds. Particles were uniformly distributed within each area. The time step was 15 min. The particles are advected by the circulation model current plus an additional (horizontal) stochastic component to represent the effects of turbulence. The latter depends on the local (time-dependent) diffusivity derived from the circulation model and is enacted in the form of a "random displacement model" (Rodean, 1996; Brickman and Smith, 2002). Because of the random component of drift, the result of a given release should be considered to be one trial of an ensemble, of which we are interested in the ensemble-averaged behaviour. As such, sufficient particles should be released to guarantee this result. The method of Brickman and Smith (2002) was used to determine that three releases (trials) of 10 000 particles were enough, when combined, to produce satisfactory drift statistics.

The circulation model flowfields are time-dependent, meaning that drift patterns depend on the yd of release. Because it was not practical to release particles every day, releases were done at 5 d intervals starting at yd 80 and ending at yd 170. This interval was chosen to safely bracket the expected egg release days from the

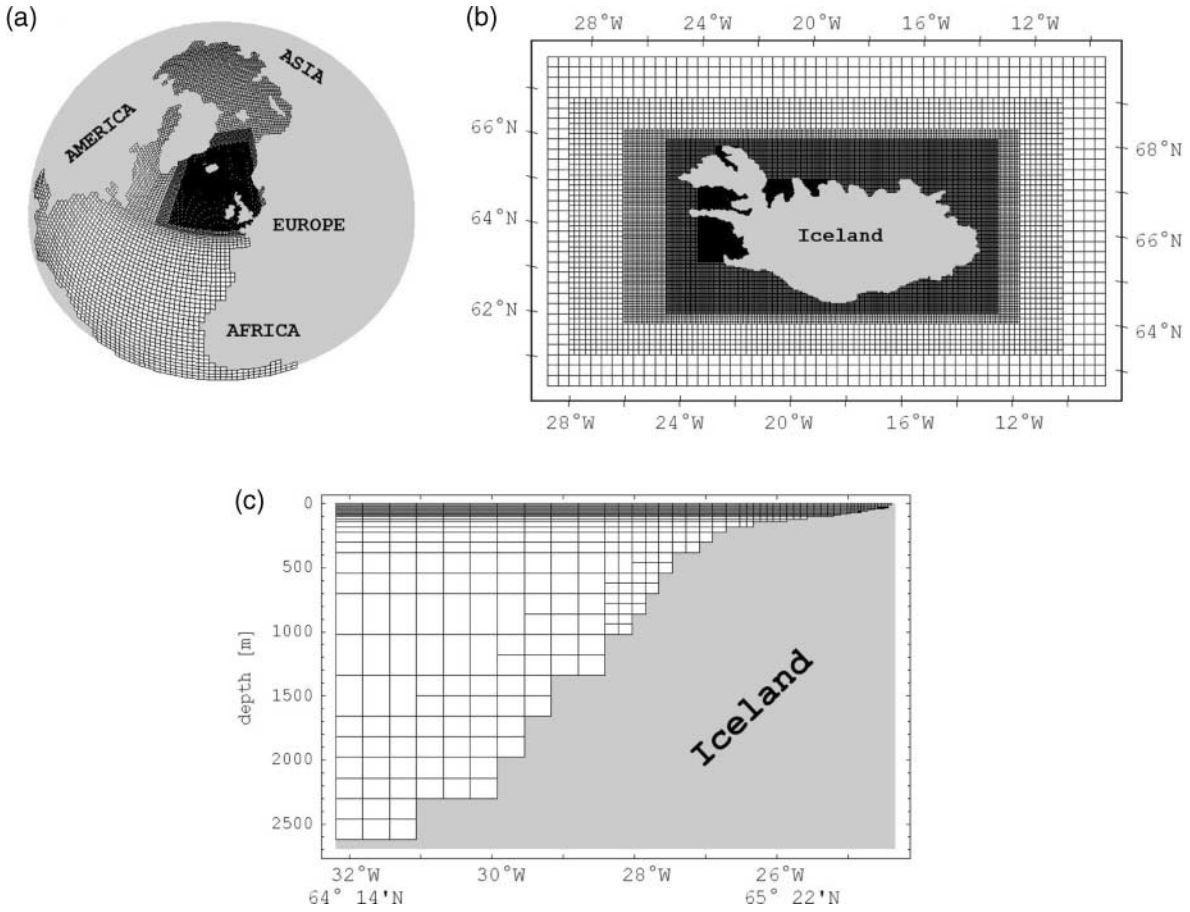

Figure 4. The adaptively refined mesh used by the circulation model. (a) The whole model domain including the North Atlantic, the Nordic Seas, and the Arctic Ocean. (b) The horizontally adaptive grid around Iceland. (c) The vertically adaptive grid west of Iceland.

various spawning grounds in Icelandic waters (Marteinsdottir and Bjornsson, 1999). Each release of particles was tracked until yd 230, i.e. the model mean survey date.

Icelandic cod eggs are positively buoyant and rise to the surface after spawning. Larvae occupy a mean depth that increases as they grow older. Larval drift studies on Georges Bank (Werner *et al.*, 1993) and Browns Bank (Brickman and Frank, 2000; Brickman *et al.*, 2001) used a time–depth algorithm deduced from field data. Unfortunately there are not sufficient egg and larval data to produce such a relationship for Icelandic cod. The algorithm used started particles 5 m deep until they hatched, after which they sank at a rate that put them at ~35 m, the mean trawl depth, after 100 larval days. Hatch time (H) was temperature-dependent (Pepin *et al.*, 1997):

$$H = 46.1\,\mathrm{e}^{-0.17T}.$$

The time–depth relationship is broadly consistent with those used by Werner *et al.* (1993) and Brickman *et al.* (2001). Experiments using different initial particle depths are reported in Brickman *et al.* (2006).

Circulation around Iceland

The circulation around Iceland is influenced by the warm Irminger and North Atlantic currents, which flow south of the country, and cold (generally cyclonic) currents to the north. This results in a clockwise circulation over the shelf, which then branches off to the east along the Iceland–Faroes Ridge (Figure 5). The collision of warm and cold water masses results in two frontal regions, one between Iceland and Greenland, the other along the Iceland–Faroes Ridge.

The output from the circulation model provides a high-resolution space/time picture of the seasonal evolution of the circulation around Iceland, essentially too much information to present compactly. Here we are interested in providing a general picture of the flow patterns in which larvae drift. To illustrate the flowfield, we use a combination of flow vectors and particle streamlines. Velocity fields are monthly averaged to eliminate the effects of individual storms. To illustrate mean drift, particle tracking is done at fixed levels with no turbulence scheme. The circulation in May is presented, because it is qualitatively similar to that in other months. Quantitative differences in drift, based on release day, are discussed below.

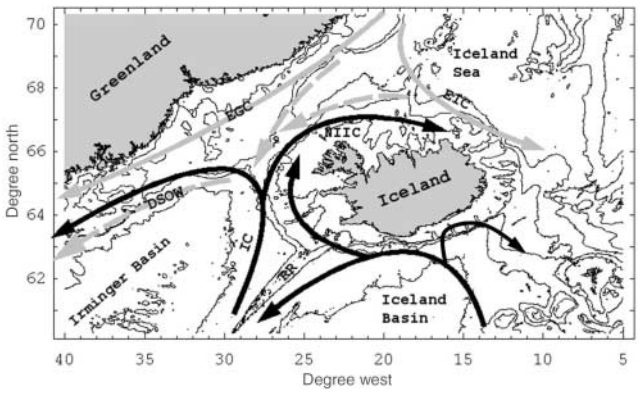

Figure 5. Schematic view of the circulation around Iceland. Black arrows signify warm Atlantic water of the Gulf Stream, grey arrows are cold currents from Arctic sources, and dashed arrows denote bottom currents. IC, Irminger current; NIIC, North Icelandic Irminger current; EGC, East Greenland current; EIC, East Icelandic current; RR, Reykjanes ridge.

The average May flowfield at 25 m (Figure 6a) shows a strong clockwise flow along the shelf-break (~600 m), starting from the southeast. The current dips around the Reykjanes Ridge and crosses isobaths west of Iceland (~28°W 66°N) to become the northern coastal current. There is evidence of flow away from Iceland towards the Faroe Islands to the east, and towards Greenland to the west. The onshelf flow is weaker and generally follows bathymetry. There is a significant eddy field, both on- and off-the-shelf, with the onshelf eddy density appearing to be related to the gradient in topography (compare the south region from 14 to 19°W against the situation over the western shelf).

Particle tracks (Figure 6b) illustrate a clockwise onshelf flow starting at ~17°W and continuing all the way to the area around the Iceland–Faroes Ridge. A counterclockwise onshelf branch point (flow bifurcation point) starts east of 17°W. Significantly, only offshelf particle releases drift towards Greenland (see Discussion).

Climatological larval drift

As mentioned above, particles are released from each of the 13 spawning grounds at 5 days intervals from yd 80 to yd 170. These release times bracket the expected spawning times, based on back-calculated total ages (Figure 2). In addition to the three-dimensional position of particles, their mean temperature and hatch time are computed and saved. All drift tracks terminate at yd 230, the mean survey date.

Figures 7 and 8 show the 30 days snapshots of particles released from representative spawning grounds on yd 125. (The layout is selected to minimize overlap of particles from the various spawning grounds.) In general, releases from the main spawning grounds (Figure 7) stay mostly inshore, with a small number of particles drifting towards Greenland, principally from spawning grounds 2 and 3. Releases from northern inshore sites show some dispersal into water >200 m deep (Figure 8; spawning grounds 4 and 5). Releases farther around the clockwise coastal circulation drift mainly out of the domain (Figure 8; spawning grounds 8 and 10). Particles released on the southeast spawning ground (12), situated near the flow bifurcation point on the south shore, drift towards the west and the east. Spawning ground 13 releases at that time drift towards the west.

One of the main goals of the study is to evaluate how the various spawning grounds contribute to the climatological age distribution (Figure 2). To do so, it is useful to characterize drift in a more compact way, in terms of the probability that an ensemble of particles released from some region (i.e. a given spawning ground) at time t_0 are found in another region at time t_1. This can be done by looking at particle positions at t_1, breaking the domain into a grid, and counting the number of particles in each grid box. We define the probability density function (pdf) for drift from a given spawning ground to a given grid cell

$$P(\text{SPG-}k, t_0; i, j, t_1) = \frac{n(i, j, t_1)}{N_k}, \qquad (2)$$

where SPG-k denotes the kth spawning ground, (i, j) the grid cell, N_k the total number of particles released from SPG-k, and

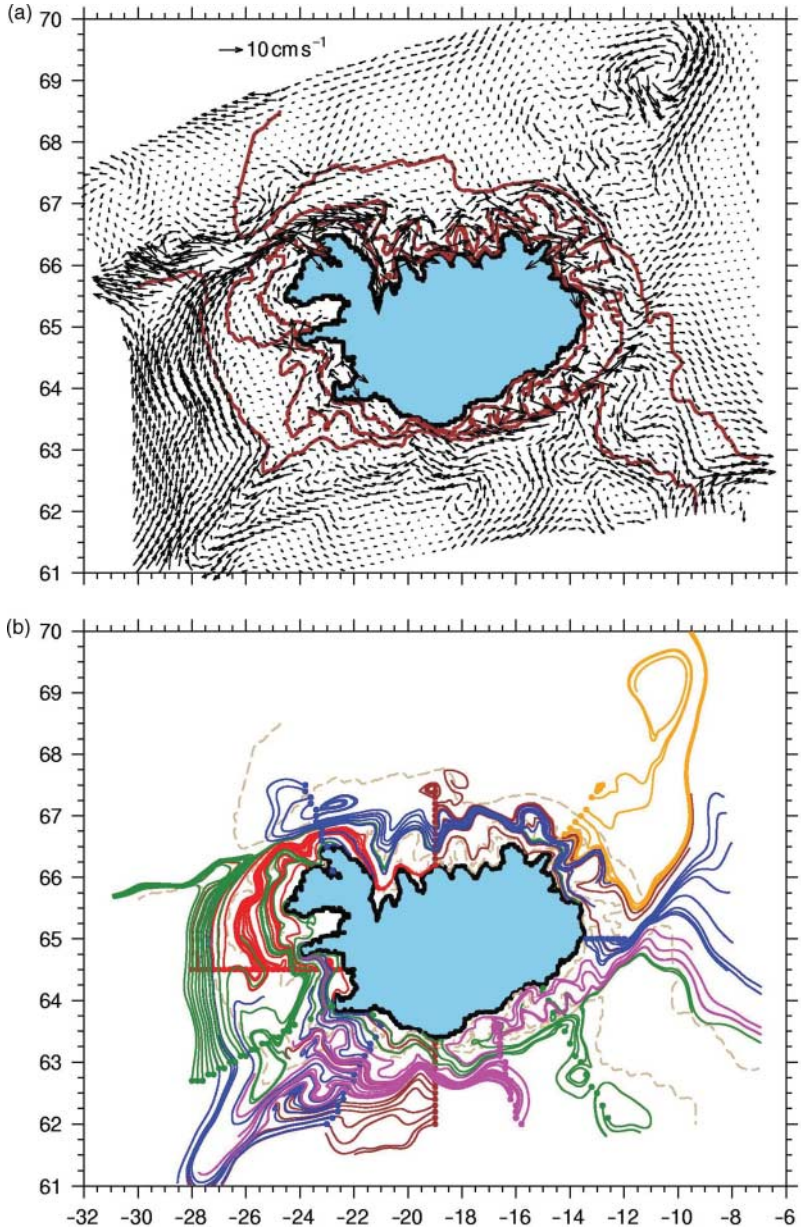

Figure 6. Average May flowfield at 25 m. (a) Velocity vectors, decimated to 15 km separation. (b) Particle drift tracks at 25 m. The symbol indicates the release position, and streamlines are 120 d long.

$n(i, j, t_1)$ the number of particles found in grid cell (i, j) at time t_1 (yd 230). In general, as the velocity field is a function of time, P(SPG-k, t_0;i, j, t_1) is a function of the time of release.

The pdf representation can be used to summarize the potential contribution of the various spawning grounds to the age-frequency distributions of juveniles surviving from the eight regions. First, note that because t_1 = yd 230, the age of a particle is completely determined by its release time. Consider an age class (A) for a given region (R_p). This age class identifies a unique release time ($t_0 = 230 - A$). The probability of drift from SPG-k to R_p is the sum of P(SPG-k, t_0; i, j,230) over grid cells $i, j \in R_p$. This operation was carried out for the four most frequent age classes of each region, for all spawning grounds. For example, spawning grounds 12, 13, and 1 are predicted to contribute to the age frequency distribution in R1, whereas spawning grounds 2 and 3, themselves contained in R1, have virtually zero probability of contributing there (Figure 9). The age distribution in R2 is most likely determined by spawning grounds 13, 1, and 2, with the oldest ages (105 and 115 days) coming from spawning grounds 1 and 13. In R3, the youngest larvae (85 days and 75 days) are most probably supplied by spawning grounds 2 and 3, although SPG-1 also contributes to the 85 d age class. In other words, the spatial age gradient between R2 and R3 (Figure 1) is predicted to be due to differences in the source regions for these larvae, with the older ones coming from the more southerly spawning grounds. The bimodal age distribution in R7 (Figure 2) is due to spawning taking place in spawning grounds 12 and 13. Inspection of the suite of probability plots for SPG-12 shows drift to the east or west plus some retention in R7, for all release times. Similar inspection for SPG-13, situated near the western boundary

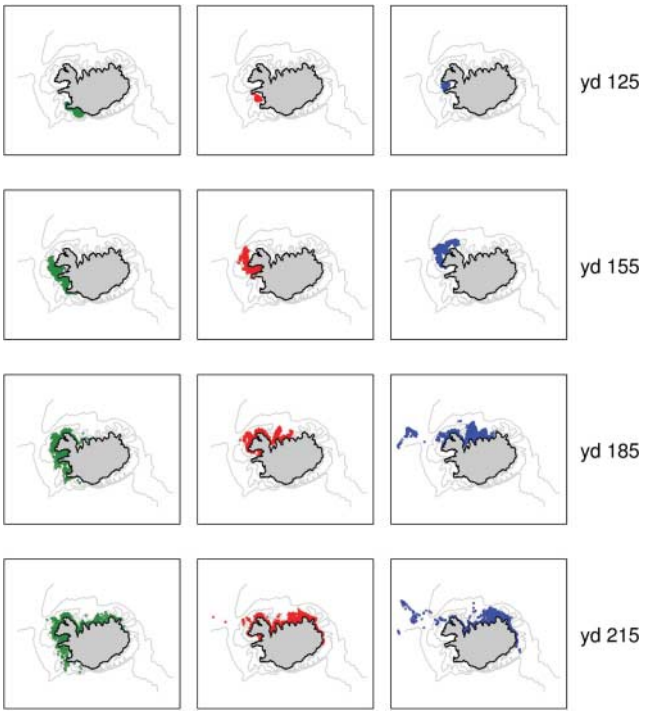

Figure 7. Particle drift from spawning grounds 1 (left column), 2 (centre column), and 3 (right column). Time proceeds in 30 d intervals from top to bottom, and initial release locations can be identified in the yd 125 panels.

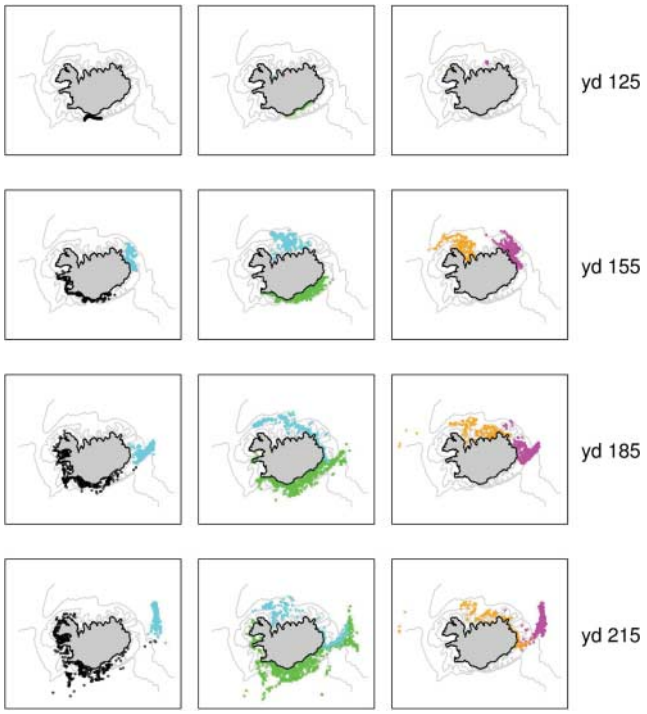

Figure 8. Particle drift from spawning grounds 10 and 13 (left column), 5 and 12 (centre column), and 4 and 8 (right column). Time proceeds in 30 d intervals from top to bottom, and initial release locations can be identified in the yd 125 panels.

of R7, shows predominately clockwise drift for release times up to yd 145, with slight retention in R7. However, this pattern changes to predominately eastward drift for releases later than yd 145 (larval ages $\leq$85 days).

The probability of drift into R8, characterized by the oldest average larval age found by the survey, is an order of magnitude lower than the other regions. Spawning grounds 2 and 3 are the most likely contributors, with SPG–4 contributing to the 115 d age class.

The general picture for regions 4–6 (R4–R6), moving clockwise in region number, is one of increasing probability of contribution from northern spawning grounds (spawning grounds $\geq$4), and decreasing probability from R1 spawning grounds (1–3). This is consistent with the prediction of Begg and Marteinsdottir (2000). The potential contribution in R6 from spawning grounds 7–10 is deceptive because the particle concentrations are offshore, where larvae are typically not found.

Begg and Marteinsdottir (2000) computed the (maximum) proportion of larvae found in a given region predicted to have come from R1 (spawning grounds 1–3), based on intersection of the back-calculated spawning distributions for the eight regions. Implicit in their analysis was (i) that R1 was responsible for most of the larvae in all regions, i.e. local contributions were minimal, and (ii) that the larval age distribution computed for R1 was due to eggs released in R1. The former assumption is reasonable in that R1 is considered to contain the bulk of the spawning-stock biomass; the latter assumption is less certain.

A drift version of the same index can be created by computing the total probability of drift, for the four most common age classes, from R1 into the other regions. This essentially assumes an equal number of eggs spawned from each region. This is unlikely to be true, but the exercise is illuminating. Figure 10 shows both the drift and the Begg and Marteinsdottir (2000) result. The general trend is similar, except for R1 and R2, but the proportions in R6 and R7 are much lower. The last result reflects the fact that there is little probability of drift from R1 to R6 and R7. The low predicted value in R1 is because there is significant probability of drift from SPG–12 and SPG–13 (R7) into the region (Figure 9). The degree to which the back-calculated spawning distribution for R1 reflects only eggs spawned in R1 is a problem requiring further investigation.

Larval drift in the context of adult population substructure

Based on recent work, there is evidence of four possible subpopulations on Iceland's south coast (Figure 11). Jonsdottir *et al.* (2002) found a genetic distinction between spawners on the Loftstadahraun and Kantur spawning grounds (in Figure 11, represented by SPG-1b and SPG-13, respectively). Marteinsdottir *et al.* (2000b), Jónsdóttir *et al.* (2006), and Petursdottir *et al.* (in press) described distinct otolith morphology and growth differences among spawners in SPG-1, demonstrating that spawning cod in SPG-1b were generally faster growing that those in the deeper areas of SPG-1c. Large, fast-growing spawning cod have also been recorded in the hatched region of SPG-12 (SPG-12b) (Gudmundsdottir *et al.*, 1998). In this section, we investigate whether there are characteristic differences in drift from those subregions on the south coast.

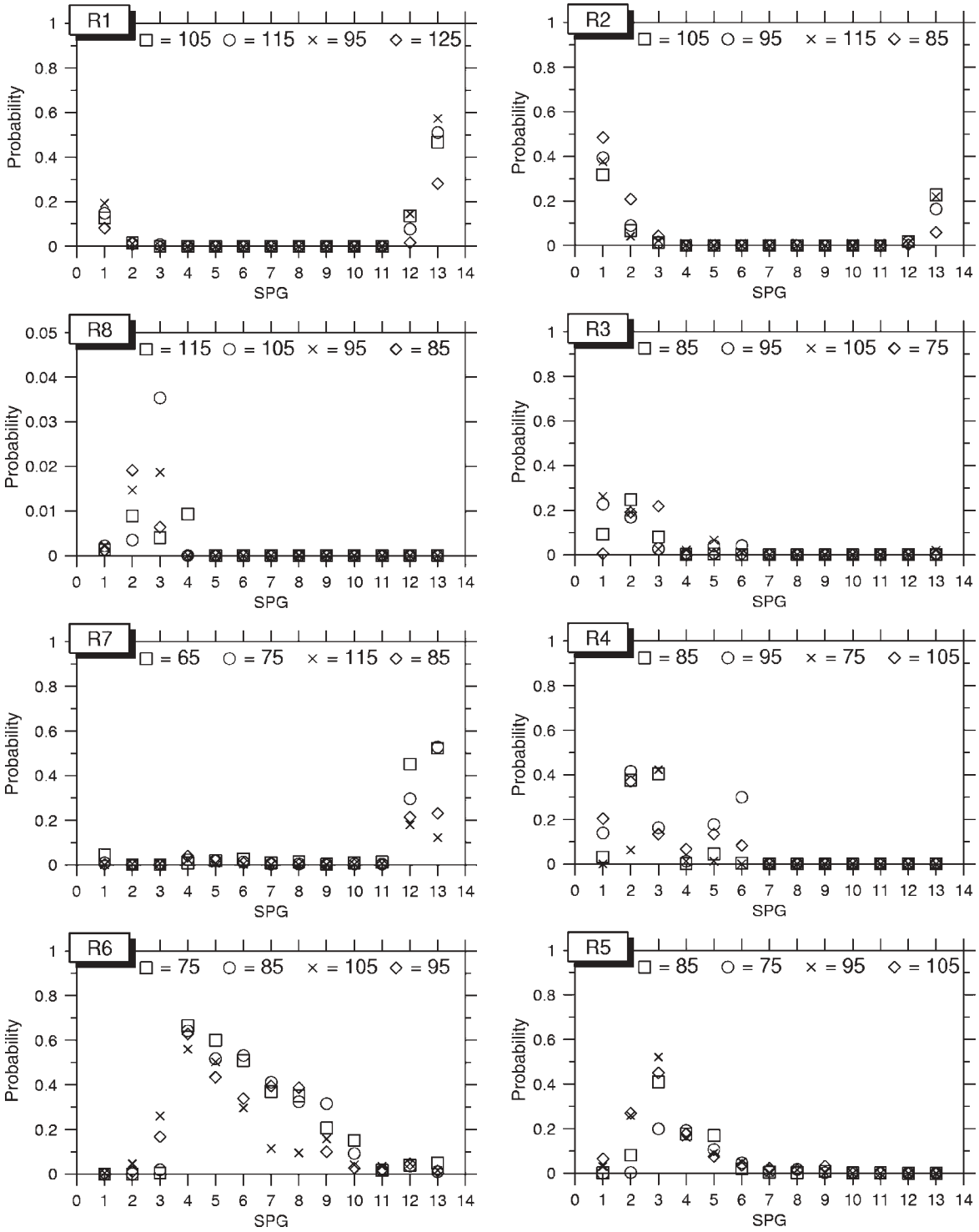

Figure 9. Probability of drift from spawning ground to region for the four most common age classes. Region number and age classes are indicated. The leftmost age is the most common.

The particle tracks from SPG-1 were analysed to see whether there were any differences in drift of particles released in shallow and deep subregions within the spawning ground (subregions a–c), and whether the temperature history of the particles was related to initial position. From the age frequency distribution of surviving 0-group cod and particle drift probability calculations (Figures 2 and 9), it can be deduced that the relevant particle release time window is yd 115–145. For this period, the histogram of mean temperature along drift paths was bimodal, with a major peak at ~6.2°C and a minor one at ~3.5°C (no figure included). This is similar to the observation (Palsson and Thorsteinsson, 2003) that there are warmer and colder groups of migrating adults

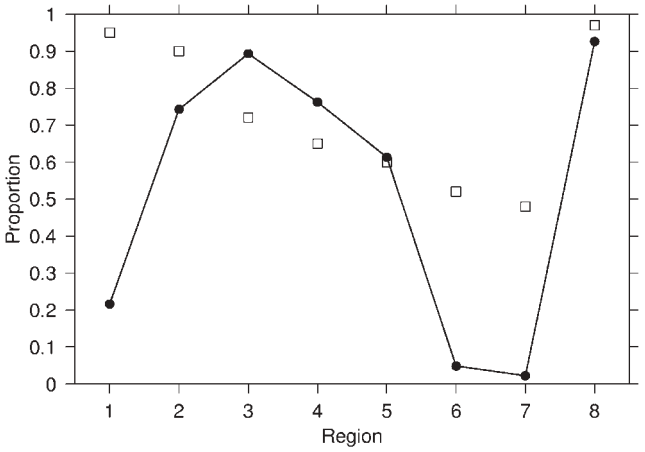

Figure 10. Proportion of larvae in the eight regions predicted to have originated in region 1 (SPG-1 to SPG-3; solid line). The Begg and Marteinsdottir (2000) prediction is included for comparison (open squares).

on the main spawning ground. However, although the colder peak was significant in probability (about 10% of particles), there was no systematic relationship between initial position and temperature. We found a slight difference in the final positions of particles released from SPG-1b than in deeper (SPG-1c) or more western (SPG-1a) spawning areas (for yd 115–145), with a higher concentration of SPG-1b particles in and south of Faxafloi Bay (~23°W 64.5°N) than from the other two areas (about two to three times greater probability; no figure included). Otherwise, the distributions showed significant overlap. Therefore, particle tracking does not indicate any strong difference in drift from subregions of SPG-1.

Adult migration from the Kantur spawning ground is typically towards the east and into deeper waters rather from shallower spawning areas (V. Thorsteinsson, Marine Research Institute, Iceland, pers. comm.). The drift probability results show that drift from SPG-13 (representing Kantur) is predominately westwards for early releases (≤yd 140, ages ≥90; see panels R1 and R2 of Figure 9), then eastwards later (panel R7 of Figure 9). Therefore, the adult migration direction corresponds to the late-spawned direction of larval drift.

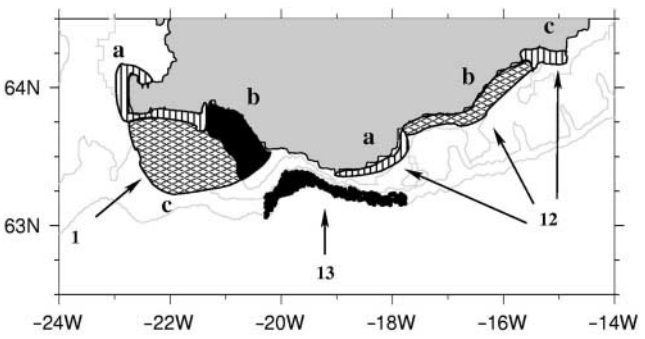

Figure 11. The southern spawning grounds, showing the (approximate) regions of known (black) or possible (cross-hatched) subpopulations. Spawning grounds 1 and 12 are divided into three subregions (SPG-1a, b, c and SPG-12a, b, c).

Drift from the subregions of SPG-12 has a complicated pattern. Particles released in SPG-12c generally drift out of Icelandic waters. The probability of a particle ending up east of 21.5°W (the eastern boundary of R7) is typically greater for releases from SPG-12b than for SPG-12a (Figure 12, solid lines) but the result is deceptive because a significant number of SPG-12b particles drift far out of R7. Therefore, although a greater fraction of western-released (SPG-12a) particles drift toward the west, the probability of retention in R7 is similar for both release locations (dashed lines of Figure 12). Thus while there are differences in drift characteristics for the subregions of SPG-12, these differences do not translate into substantially different contributions to the 0-group distribution in R7. With respect to the 0-group distribution in R1, the western part of SPG-12 is the only potential contributor (except for yd 120 releases; see solid lines of Figure 12).

Discussion

We investigated larval drift from 13 spawning grounds in Iceland waters (Figure 3), with the goal of understanding how various spawning areas contribute to the climatological distribution of 0-group cod larvae. Larvae were modelled as vertically migrating particles drifting in flowfields produced by a high-resolution numerical circulation model focused specifically on Icelandic waters.

Particle-tracking results support the general picture of a clockwise drift "conveyor belt" along the shelf, starting near the southernmost spawning grounds. There is some offshelf dispersion, principally along the Iceland–Faroes Ridge, but also towards Greenland. The farther a spawning ground is along this conveyor, the farther downstream its larvae will drift.

In reference to the climatological 0-group distribution (Figures 1 and 2), the observed spatial gradient in age is likely attributable to differences in the spawning location of the larvae, the older larvae originating in SPG-13, SPG-1, and SPG-2, whereas the younger larvae have a more northern origin (SPG-2

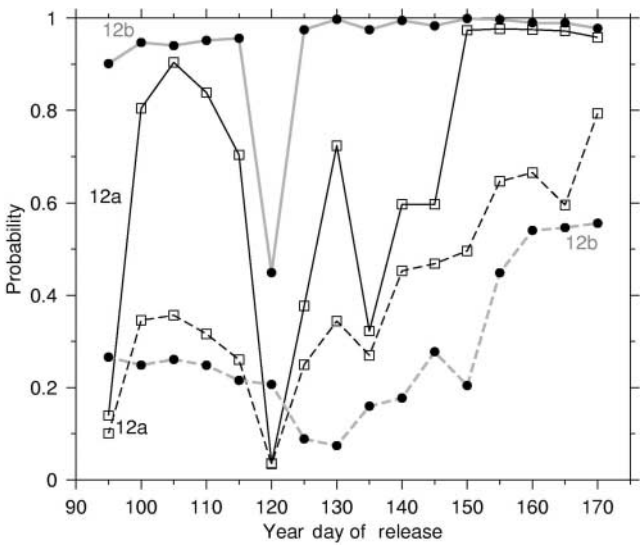

Figure 12. Drift probabilities for releases from SPG-12a (black lines, squares) and SPG-12b (grey lines, dots). Solid lines are probabilities of ending up east of 21.5°W. Dashed lines are probabilities of retention in R7.

and SPG-3). The younger larvae along the northern shelf come from spawning grounds progressively farther along the conveyor belt (SPG-4 to SPG-7). Larvae released from the northeastern spawning grounds (SPG-8 to SPG-11) drift mainly out of Icelandic waters, suggesting little contribution from those spawning grounds to the climatological 0-group distribution. In general, the contribution from the main spawning grounds in the southwest is predicted to decrease with clockwise distance from the source region. This result is similar to that predicted by Begg and Marteinsdottir (2000) from consideration of the back-calculated spawning duration curves, although there are differences (Figure 10). The bimodal age distribution observed in R7 is due exclusively to eggs released in SPG-13 and SPG-12 along the southern shelf, a finding that would not have been predicted from spawning duration curves alone.

The above deductions implicitly assume that all spawning grounds release the same number of eggs. As a rough guide, it is expected that the northern spawning grounds (SPG-4 to SPG-11) contribute $\leq$10% of spawned eggs in total, SPG-1 is responsible for $\sim$20–30%, and the rest of the southern spawning grounds (SPG-2, SPG-3, SPG-12, SPG-13) contribute potentially equal numbers (Brickman *et al.*, 2006). Consideration of these weightings does not influence our basic conclusions.

The probability plot for spawning grounds and regions (Figure 9) shows more than an order of magnitude less probability of drift to R8 (towards Greenland) than the other regions. This could be because the climatological flowfield does not model interannual variability, so that if the data show drift to R8 in "events", then the climatological drift could not simulate this. Inspection of the R8 abundance data does in fact show that Iceland–Greenland larval drift is episodic, with major peaks in 1973, 1984, 1997, and 1999, and minor peaks in 1981 and 1987 (Schopka, 1993; Begg and Marteinsdottir, 2000; unpublished results of the METACOD project). The mean abundance is 2.75 larvae per kilometre, with an s.d. of 37. If the peak years are eliminated, the mean abundance is 0.16 with an s.d. of 0.88, indicating the extent to which the R8 data are dominated by episodic years. Note that the studies of West Greenland cod also support episodic immigration of juveniles from Iceland (Storr-Paulsen *et al.*, 2003).

Particle tracking indicates virtually no drift into waters deeper than 200 m, whereas abundance data (Figure 1) show evidence of drift offshelf (deeper than 600 m). This could indicate that the circulation model solutions are not sufficiently dispersive, or be due to the lack of deep water particle release sites, whereas gillnet and trawl data (not shown) indicate some possible spawning in deeper water. Figure 6 generally supports the picture of deeper releases staying in deeper water, so perhaps the source regions for the deeper 0-group cod are small shelf-break spawning aggregations not represented in our particle-tracking model. Another possibility is that larvae disperse more as they grow older, because of the interaction of increasing swimming capability and turbulence. This can be modelled by adding an age-dependent random drift to particles. Whatever the reason, however, this problem requires more investigation.

We looked at drift from regions on the south coast corresponding to known or possible subpopulation spawning grounds, to evaluate whether these spawning grounds are associated with distinct drift patterns. For the Loftstadahraun and Kantur spawning areas (SPG-1b and SPG-13; Figure 11), representing spawning aggregations of different genetic frequencies as well as life history properties, we found larval drift to be predicted in separate directions if most spawning from Kantur was after yd 140. If this is the case, then larval drift from Kantur is in the same direction as adult feeding migration (eastwards), suggesting that Kantur juveniles recruit to their stock by mixing with adult fish co-occurring in a joint nursery/feeding ground (as suggested by Rose, 1993, for northern cod). However, this idea is complicated by the fact that larvae from SPG-12 are predicted to share the same general nursery area. The extent of mixing in this southeastern nursery region, and how this relates to adult population structure, requires more research.

Larval drift from subregions of the main spawning ground showed weak spatial differentiation. The mean larval drift temperature did exhibit a bimodal distribution. However, this was not associated with specific release sites, but rather was the result of the statistics of randomized drift in a space- and time-varying flowfield. A bimodal temperature distribution supports the finding from data storage tagging of adults (Palsson and Thorsteinsson, 2003). The genetic properties of the adult population in SPG-1 have currently not been resolved, but these aggregations do segregate into a sort of size-based pecking order, with the largest fish inshore and smaller adults in deeper water (Marteinsdottir *et al.*, 2000b; Petursdottir, *et al.*, in press). It is interesting to speculate that this size-based adult structure is the result of temperature-dependent differences in growth starting at the larval phase. In such a scenario, it makes no difference where in SPG-1 a cod is spawned, but if its drift history is "colder", then it would grow more slowly and end up segregated into the deeper (smaller) adult subpopulation.

We have shown that particle tracking can aid in understanding basic features of the climatological larval distribution in Iceland waters, as well as adding to the discussions of population substructure. The pdf approach used in this study is useful but is ultimately limited, because it does not account for the relative spawning-stock biomass on each spawning ground. Biophysical models take into account the number of eggs spawned and the mortality along drift trajectories to predict absolute numbers of surviving larvae. Ultimately, application of such a model is required to understand the observed abundance and the age distributions and to address outstanding questions such as the numerical contribution of juveniles from the various spawning grounds and the extent of mixing in nursery areas.

Acknowledgements

This project was partly funded by the EU (METACOD—project Q5RS–2001–00953), the Icelandic Research Council, and the Icelandic Ministry of Fisheries. The manuscript benefited from the comments of three anonymous reviewers.

References

Backhaus, J. O. 1985. A three-dimensional model for the simulation of shelf sea dynamics. Deutsche Hydrographische Zeitschrift, 38: 165–187.

Begg, G. A., and Marteinsdottir, G. 2000. Spawning origins of pelagic juvenile cod *Gadus morhua* inferred from spatially explicit age distributions: potential influences on year-class strength and recruitment. Marine Ecology Progress Series, 202: 193–217.

Begg, G. A., and Marteinsdottir, G. 2003. Spatial partitioning of relative fishing mortality and spawning stock biomass of Icelandic cod. Fisheries Research, 59: 343–362.

Brickman, D., and Frank, K. T. 2000. Modelling the dispersal and mortality of Browns Bank egg and larval haddock *Melanogrammus*

aeglefinus. Canadian Journal of Fisheries and Aquatic Sciences, 57: 2519–2535.

Brickman, D., Shackell, N. L., and Frank, K. T. 2001. Modelling the retention and survival of Browns Bank haddock larvae using an early life stage model. Fisheries Oceangraphy, 10: 284–296.

Brickman, D., and Smith, P. C. 2002. Lagrangian stochastic modelling in coastal oceanography. Journal of Atmospheric and Oceanic Technology, 19: 83–99.

Brickman, D., Taylor, L., Gudmundsdottir, A., and Marteinsdottir, G. 2006. Optimized biophysical model for Icelandic cod larvae. Fisheries Oceanography. To appear.

Canino, M. F., and Bentzen, P. 2004. Evidence for positive selection at the Pantophysin (Pan I) locus in walleye pollock, *Theragra chalcogramma*. Molecular Biology and Evolution, 21: 1391–1400.

Gudmundsdottir, A., Thorsteinsson, V., and Marteinsdottir, G. 1998. Stofnmæling hrygningarþorsks med þorskanetum 1998. [Gillnet survey of spawning cod in Icelandic waters in 1998.] Technical Paper Marine Research Institute, 71. 19 pp.

Harms, I. H., Backhaus, J. O., and Hainbucher, D. 1999. Modelling the seasonal variability of circulation and hydrography in the Iceland–Faeroe–Shetland overflow area, ICES Document CM 1999/L: 10. 8 pp.

Harms, I. H., Heath, M., Bryant, A., Backhaus, J. O., and Hainbucher, D. 2000. Modelling the northeast Atlantic circulation—implications for the spring invasion of shelf regions by *Calanus finmarchicus*. ICES Journal of Marine Science, 57: 1694–1707.

Harms, I. H., Hübner, U., Backhaus, J. O., Kulakov, M., Stanovoy, V., Stepanets, O., and Kodina, L., *et al.* 2003. Salt intrusions in Siberian river estuaries: observations and model experiments in Ob and Yensiei. *In* Siberian River Runoff in the Kara Sea: Characterisation, Quantification, Variability and Environmental Significance. Proceedings in Marine Science, 6, 27–46. Ed. by R. Stein, K. Fahl, D. K. Fütterer, E. M. Galimov, and O. V. Stepanets. Elsevier, Amsterdam. 484 pp.

Heath, M., and Gallego, A. 1998. Bio-physical modelling of the early life stages of haddock, *Melanogrammus aeglefinus*, in the North Sea. Fisheries Oceanography, 7: 110–125.

Hinrichsen, H-H., Mollmann, C., Voss, R., Koster, F. W., and Kornilovs, G. 2002. Biophysical modeling of larval Baltic cod (*Gadus morhua*) growth and survival. Canadian Journal of Fisheries and Aquatic Sciences, 59: 1858–1873.

Houde, E. D. 1997. Patterns and trends in larval-stage growth and mortality of teleost fish. Journal of Fish Biology, 51 (Suppl. A): 52–83.

Jónsdóttir, I. G., Campana, S. E., and Marteinsdottir, G. 2006. Otolith shape and temporal stability of spawning groups of Icelandic cod (*Gadus morhua L.*). ICES Journal of Marine Science, 63: 1501–1512.

Jonsdottir, O. D. B., Imsland, A. K., Danielsdottir, A. K., and Marteinsdottir, G. 2002. Genetic heterogeneity and growth properties of different genotypes of Atlantic cod (*Gadus morhua* L.) at two spawning sites off south Iceland. Fisheries Research, 55: 37–47.

Khokhlov, A. M. 1998. Fully threaded tree algorithms for adaptive refinement fluid dynamics simulations. Journal of Computational Physics, 143: 519–543.

Logemann, K., Backhaus, J. O., and Harms, I. H. 2004. SNAC: a statistical emulator of the north-east Atlantic circulation. Ocean Modelling, 7: 94–110.

Logemann, K., and Harms, I. 2006. High resolution modelling of the north Icelandic Irminger Current (NIIC). Ocean Science Discussions, 3: 1149–1189.

Marteinsdottir, G., and Bjornsson, H. 1999. Time and duration of spawning of cod in Icelandic waters. ICES Document CM 1999/Y: 34. 22 pp.

Marteinsdottir, G., Gunnarsson, B., and Suthers, I. M. 2000a. Spatial variation in hatch date distributions and origins of pelagic juvenile cod in Icelandic waters. ICES Journal of Marine Science, 57: 1182–1195.

Marteinsdottir, G., Gudmundsdottir, A., Thorsteinsson, V., and Stefánson, G. 2000b. Spatial variation in abundance, size composition and viable egg production of spawning cod (*Gadus morhua* L.) in Icelandic waters. ICES Journal of Marine Science, 56: 824–830.

Marteinsdottir, G., Ruzzante, D., and Neilsen, E. O. 2005. History of North Atlantic cod stocks. ICES Document CM 2005/AA: 19. 17 pp.

Palsson, O. K., and Thorsteinnsson, V. 2003. Migration patterns, ambient temperature, and growth of Icelandic cod (*Gadus morhua*): evidence from storage tag data. Canadian Journal of Fisheries and Aquatic Sciences, 60: 1409–1423.

Pepin, P., Orr, D. C., and Anderson, J. T. 1997. Time to hatch and larval size in relation to temperature and egg size in Atlantic cod (*Gadus morhua*). Canadian Journal of Fisheries and Aquatic Sciences, 54 (Suppl. 1): 2–10.

Petursdottir, G., Begg, G. A., and Marteinsdottir, G. 2006. Discrimination between Icelandic cod (*Gadus morhua*) populations from adjacent spawning areas based on otolith growth and shape. Fisheries Research, 80: 182–189.

Pogson, G. H. 2001. Nucleotide polymorphism and natural selection at the Pantophysin (Pan I) locus in the Atlantic cod, *Gadus morhua* (L.). Genetics, 157: 317–330.

Rodean, H. C. 1996. Stochastic Lagrangian models of turbulent diffusion. Meteorological Monographs, 48, American Meteorological Society, Massachusetts, USA. 84 pp.

Rose, G. A. 1993. Cod spawning on a migration highway in the North-West Atlantic. Nature, 366: 458–461.

Röske, F. 2001. An atlas of surface fluxes based on the ECMWF re-analysis—a climatological dataset to force global ocean general circulation models. 31. (http://www.mpimet.mpg.de/Depts/Klima/natcli/omip.html).

Saemundsson, K. H. 2005. Dispersal of juvenile cod in Icelandic waters. MSc thesis, University of Iceland. 118 pp.

Schopka, S. A. 1993. The Greenland cod (*Gadus morhua*) at Iceland 1941–1990 and their impact on assessments. NAFO Scientific Council Studies, 18: 81–85.

Steele, M., Morley, R., and Ermold, W. 2001. PHC: a global ocean hydrography with a high quality Arctic Ocean. Journal of Climate, 14: 2079–2087.

Stefánsson, G., and Palsson, O. K. 1997. BORMICON. boreal migration and consumption model. Technical Paper, Marine Research Institute, 58. 223 pp.

Storr-Paulsen, M., Wieland, K., Hovgard, H., and Ratz, H. J. 2003. The stock structure of Atlantic cod (*Gadus morhua*) in West Greenland waters: implications of transport and migration. ICES Document CM 2003/O: 06. 20 pp.

Werner, F. E., Page, F. E., Lynch, D. R., Loder, J. W., Lough, R. G., Perry, R. I., and Greenberg, D. A., *et al.* 1993. Influences of mean advection and simple behavior on the distribution of cod and haddock early life stages on Georges Bank. Fisheries Oceanography, 2: 43–64.

doi:10.1093/icesjms/fsl019